Propane Oxidative Dehydrogenation on $BiP_{1-X}V_XO_4$ Supported Silica Catalysts

Ouchabi, M'barka
Laboratory of Catalysis and Corrosion of Materials, Chouaïb Doukkali University, Faculty of Sciences El Jadida, BP. 20, El Jadida, MOROCCO

Loulidi, Ilyasse*+
Laboratory of Chemistry and Biology Applied to the Environment, Faculty of Sciences, Moulay Ismail University, BP 11,201-Zitoune, Meknes, MOROCCO

Agunaou, Mahfoud
Laboratory of Catalysis and Corrosion of Materials, Chouaïb Doukkali University, Faculty of Sciences El Jadida, BP. 20, El Jadida, MOROCCO

ABSTRACT: *The molecularly dispersed $BiP_{1-x}V_xO_4/SiO_2$ supported oxides, with x varying from 0 to 1, were prepared by impregnation of Bismuth, Phosphorus, and Vanadium on silica. Their structures have been characterized by different techniques: X-ray diffraction, Raman spectroscopy, Temperature-Programmed Reduction of catalysts in H_2 (H_2-TPR), and methanol oxidation reaction. This very sensitive technique provided us with relevant information on the nature of the active sites (acid-base and redox) on the surface of the catalysts. The results of the characterization show the structural evolution of the vanadium species of the isolated crystallites from V_2O_5 for x =0.3 and x =0.5, to $BiVO_4$, with the disappearance of $BiPO_4$, with the increase of the vanadium content from x=0.5 to x = 1. The oxidation of methanol showed the basic properties of the $BiPO_4/SiO_2$ catalyst, by the formation of carbon dioxide as the major product of the reaction. The substitution of phosphorus with vanadium promotes the formation of formaldehyde, confirming the presence of redox sites on these substituted catalysts. These catalysts were examined in the Oxidative dehydrogenation (ODH) of propane. For $x \geq 0.5$, the dispersed $BiVO_4$ exhibited significant activity in propane ODH than the $BiPO_4$ and V_2O_5 crystallites, with good selectivity to propylene and acrolein, consistent with their high reducibility confirmed by H_2-TPR, and the presence of redox sites shown by the oxidation of methanol. The catalyst with x = 0 was less selective for propylene due to the favorable combustion of propylene during its formation. Such an understanding of the intrinsic catalytic properties of the $BiP_{1-x}V_xO_4/SiO_2$ oxides and in particular, the $BiPO_4$ and $BiVO_4$ crystallites provides new information on the structural requirements of the propane ODH reaction, beneficial for the design of more efficient Bi-P-V-O based catalysts for propylene and acrolein production.*

KEYWORDS: *Oxidative dehydrogenation; Propane; Propylene; Acrolein; $BiP_{1-x}V_xO_4/SiO_2$.*

* *To whom correspondence should be addressed.*
+ *E-mail: il.loulidi@gmail.com*
1021-9986/2023/1/79-89 11/$/6.01

INTRODUCTION

The direct conversion of light alkanes into high-value products is one of the most difficult challenges in catalytic chemistry because of the very high stability of these short-chain alkanes. The development of a satisfactory process could allow the use of natural gas as a feedstock for the production of intermediate chemicals conventionally obtained from petroleum. Among these reactions, the production of propylene and acrolein by Oxidative DeHydrogenation (ODH) of propane would be a good way to use these inexpensive molecules for purposes other than energy production (automotive propulsion or heat production). Recently, the selective oxidation of propane to propylene and acrolein is gaining more and more interest due to its application prospects and the importance of theoretical research. Numerous studies on the direct oxidation of propane have been reported [1–3], in which V-Mg-O, Mo-V-Te-Nb-O, and Ag-Bi-Mo-V-O catalysts showed superior activity and selectivity [4–7]. The activation process of propane generally follows Mars van Krevelen mechanisms. Current research has proven that V-O, V-P-O and Bi-P-V-O catalysts contain all the key catalytic elements required [8–14] for better activity and selectivity in the Oxidative dehydrogenation (ODH) reaction. In addition, metal oxides supported by SiO_2, Al_2O_3, or TiO_2 have been studied [15–19], due to better dispersion of active species or higher specific surface area. Our first study on Oxidative dehydrogenation (ODH) was performed on unsupported $BiP_{1-x}V_xO_4$ catalysts, promising results found in this study were published [8]. However, such an improvement in the performance of $BiP_{1-x}V_xO_4$ crystallites prompts us to study the dispersion of these most active and selective crystallites on silica and their catalytic consequence in the Oxidative dehydrogenation (ODH) of propane. Therefore, in this work, we prepare thermally stable Bi-P-V-O catalyst crystallites on SiO_2 support. The resulting catalysts were characterized by several techniques to describe the structural evolution of molecular species on the support surface as a function of V content. The redox active sites present on the support surface were identified as the most important ones. The redox active sites present on the surface of the supported catalysts were analyzed by methanol oxidation to estimate their roles in propane ODH [20]. In addition, we used temperature-programmed reduction of the catalysts in H_2 (H_2-TPR) to study the influence of reducible properties on the catalytic activity. The catalytic behavior of these solids in propane ODH was determined using a flow reactor equipped with on-line chromatographic analysis. An important part of the work was to establish the influence of the structure of the dispersed molecules and the nature of the active sites present on the activity and selectivity of the products obtained.

EXPERIMENTAL SECTION

Catalyst preparation

A series of $BiP_{1-x}V_xO_4/SiO_2$ catalysts were prepared using a silica support, and with a P/V mole fraction of 9/1, 8/2, 7/3, 6/4, 5/5, 4/6, 3/7, 2/8 and 1/9 (x = 0, 0.1, 0.2, 0.3, 0.4, 0.5, 0.6, 0.7, 0.8, 0.9, 1). The silica used is of the type: aerosil 380, degussa. It is a hydrophilic fumed silica with a specific surface of 320 m^2/g. These catalysts were prepared by the successive wet impregnation technique using a solution of $Bi(NO_3)_3.5H_2O$, NH_4VO_3 and H_3PO_4. According to the following mechanism, a solution of bismuth nitrate $Bi(NO_3)_3.5H_2O$ was melted in a predetermined amount of distilled water and then impregnated on a well-defined amount of silica. The impregnated Bi/SiO_2 catalysts were dried for 12 hours at a temperature of 393K, then calcined under a stream of air at 673K for 4 hours. A second impregnation on Bi/SiO_2 was performed using an aqueous solution of NH_4VO_3 and H_3PO_4. Then, the impregnated catalysts were dried again for 12 h at 393K and calcined under an air stream at 673K for 4 hours.

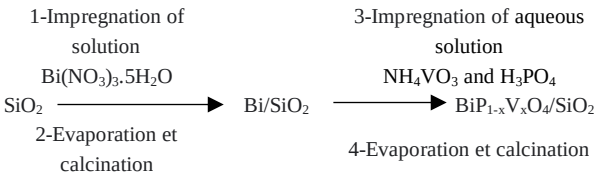

Catalyst characterization

X-Ray Diffraction: XRD was carried out using a Siemens (D500) Diffractometer and Monchromated CuK radiation ($K\lambda_\alpha$ = 1.5406Å).

Raman spectroscopy: Raman spectra were recorded at room temperature on a Perkin Elmer system 2000R, equipped with a Nd:Yag near IR laser, Neodymium doped with ytrium-aliminum producing radiation at 1064 nm. Detector in Ga As. The control of the spectrophotometer and the data acquisition are done with a microcomputer.

The frequencies are assigned using data from the literature.

Temperature-programmed reduction of catalysts in H_2 (H_2-TPR) profiles were obtained by injecting a H_2/Ar through the sample (about 70mg). The temperature was increased from 25°C to 900°C at a rate of 5°C/min, and the amount of H_2 consumed was determined with a thermo conductivity detector.

Methanol oxidation

The methanol oxidation was studied by the flow method, as described elsewhere [20]. The composition of the reactant feed $CH_3OH/O_2/H_2$ was in molar ratio 7.1/15.5/77.4, corresponding to a partial pressure of 54 torr. The reactant mixture was obtained by flowing an O_2/He mixture through a methanol saturator maintained at 10°C. The overall flow rate and the amount of catalyst were adjusted in order to secure a moderate methanol conversion, not exceeding 10%. The reaction rates are expressed as the methanol consumption for the formation of a given product. The reaction temperature was fixed at 250°C.

Propane ODH reactions

Catalyst testing: The catalytic measurements in ODH reaction were performed at atmospheric pressure on the temperature at 480°C, by a conventional continuous flow quartz reactor. The molar composition of the reaction mixture was C_3H_8/O_2/He = 8/8/1. All the tests were carried using 1g of catalyst.

RESULTS AND DISCUSSION

Structures of $BiP_{1-x}V_xO_4/SiO_2$ catalysts

Fig. 1, shows the XRD patterns of the $BiP_{1-x}V_xO_4/SiO_2$ catalysts with different V contents ($0 \leq x \leq 1$). The diffraction peaks at 2θ of 19° and 29°, which are the characteristic feature of $BiVO_4$ (reference code 01-075-2480 shown in Table I), were slightly visible for the x = 0.7 catalyst, and they became stronger as the V content increased ($x \geq 0.7$), suggesting the formation of crystalline $BiVO_4$ in the catalysts with higher V contents. However, $BiVO_4$ and $BiPO_4$ crystallite was not identified by XRD for the catalysts with x = 0.3 and x = 0.5, on the other hand we note, a weak dispersion of the V_2O_5 species (reference code 01-075-0457 shown in Table I) on the surfaces of this catalysts. In addition, for solids with x = 0 and x = 0.1. A slight dispersion of the $BiPO_4$ ximengite species observed, with total disappearance of the species containing vanadium. In comparison with our previous study made on unsupported $BiP_{1-x}V_xO_4$ catalysts (Figs. 2 and 3), poor crystallization may be due to the amorphous structure of the silica support (Fig. 2) [8,21–23].

These XRD results are consistent with the following Raman spectra. As shown in Fig. 4, a Raman band at 837 cm^{-1}, characteristic of the symmetrical stretching vibration V-O [24]. Moreover, the bands at 328 and 211 cm^{-1}, corresponding to the O-V-O deformation frequencies, are only observed for catalysts with $x \geq 0.7$, suggesting the dominant presence of VO_4 tetrahedral in $BiP_{1-x}V_xO_4/SiO_2$ on both catalysts [25]. As the V content decreases, the band at 837 cm^{-1} disappears completely when the $x \leq 0.5$. In addition, for the catalysts with x= 0.3 and x = 0.5, no bands corresponding to the V_2O_5 structure appear in the region at 995; 680-690; 407 and 281 cm^{-1} corresponding to V_2O_5 species, which is in agreement with the above mentioned XRD results showing weak crystallization and dispersion of V_2O_5 crystallites on silica.

On the other hand, there were no bands around 970 cm^{-1} and 1040 cm^{-1}, which correspond to the Raman characteristics of PO_4 tetrahedral for x = 0 and x = 0.3, respectively [26], indicating a low dispersion of $BiPO_4$ in these catalysts, confirming previous X-Ray results of these catalysts.

Reducibility of $BiP_{1-x}V_xO_4/SiO_2$ catalysts

The catalyst reducibility of $BiP_{1-x}V_xO_4/SiO_2$ catalysts was probed by H_2-TPR, as shown in Fig. 5, the catalysts with x > 0 exhibited the similar H_2-TPR characteristic with a broad reduction peak between 873 K and 973K, corresponding to the reduction from V^{5+} to V^{3+} in H_2 [27–29]. An increase in the V content shifted the temperature peak from 913K for x = 0.3 to 853K for x = 1 (as indicated by the dotted line). However, in the absence of the species vanadium a small reduction observed for x = 0 from Bi^{2+} to Bi°. Thus, the initial H_2 reduction steps, rather than the peak temperatures of the H_2-TPR curves for $BiP_{1-x}V_xO_4/SiO_2$ catalysts, are most relevant to the redox cycles required for the ODH of propane. The rate of H_2 consumption (peak area) decreased continuously by decreasing the V content from x = 1 to x = 0, suggesting lower reducibility of the $BiPO_4/SiO_2$ catalyst, this is due to low dispersion of $BiPO_4$ species on the silica support proven by X-ray diffraction. This trend parallels that of the measured propane conversion rates, as shown below.

Table I: The different phases identified by XRD of prepared catalysts.
Initial conditions: All catalysts are calcined at 650°C. The 2θ were scanned from 10 to 70°.

x	Sample	Identified phases	Reference code
0	$BiPO_4/SiO_2$	$BiPO_4$ (Ximengite)	00-001-0812
0.1	$BiP_{0.9}V_{0.1}O_4/SiO_2$	$BiPO_4$ (Ximengite)	00-001-0812
0.3	$BiP_{0.7}V_{0.3}O_4/SiO_2$	V_2O_5	01-075-0457
0.5	$BiP_{0.5}V_{0.5}O_4/SiO_2$	V_2O_5 $BiVO_4$ (Fergusonite)	01-075-0457 01-075-2480
0.7	$BiP_{0.3}V_{0.7}O_4/SiO_2$	$BiVO_4$ (Fergusonite)	01-075-2480
0.9	$BiP_{0.1}V_{0.9}O_4/SiO_2$	$BiVO_4$ (Fergusonite)	01-075-2480
1	$BiVO_4/SiO_2$	$BiVO_4$ (Fergusonite)	01-075-2480

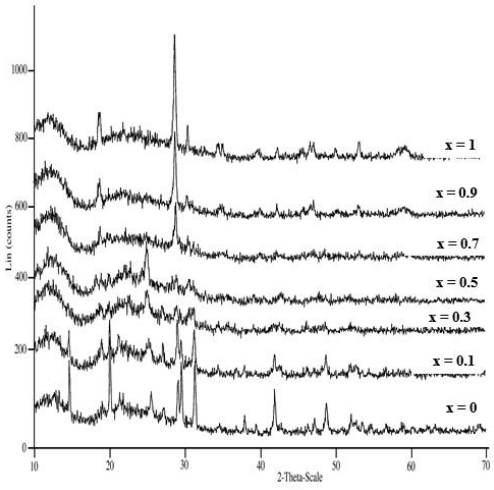

Fig. 1: XRD profiles of $BiP_{1-x}V_xO_4/SiO_2$ catalysts.

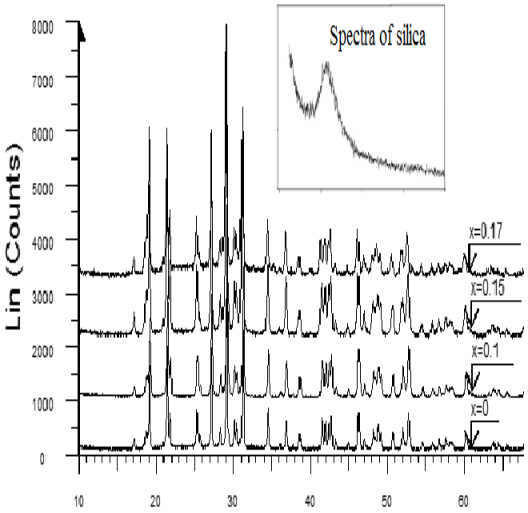

Fig. 2: X-ray diffraction spectra of unsupported $BiP_{1-x}V_xO_4$ catalysts isotype to $BiPO_4$ [21–23].

Identification of the nature of the active sites

The active redox sites in the silica supported $BiP_{1-x}V_xO_4$ catalysts were quantified by the methanol oxidation reaction [20,30]. The main products detected were formaldehyde, methyl formate, and carbon dioxide, whereas dimethyl ether and methylal are almost absent in the methanol oxidation processes for all catalysts with $0 \leq x \leq 1$, as shown in the Table II. This result is consistent with the oxidation of methanol on unsupported $BiP_{1-x}V_xO_4$ [8], producing formaldehyde with a selectivity higher than 90%. Only one exception was noticed for x=0, which presents a high selectivity in CO_2 (64%), while in our previous work on unsupported $BiP_{1-x}V_xO_4$, we found a very good selectivity in dimethyl ether (88%) for x = 0.

The nature of the catalytic sites is rarely known, nevertheless, the structural sensitivity of the methanol oxidation reaction allows the identification of different site structures capable of selectively forming a single product. As mentioned in Table II, the selective formation of methyl formate can be attributed to a dual site comprising a dehydrogenating redox site and a basic site, whereas the formation of formaldehyde requires only a dehydrogenating redox site. A significant change in the selectivity of methyl formate or the ratio of methyl formate to formaldehyde will indicate a change in the basicity of the catalyst. Similarly, the selective formation of dimethyl ether and carbon dioxide are attributed successively to the presence of strong acidic sites and strong basic sites, without the involvement of active redox sites. Formaldehyde, which is formed by the Mars-van Krevelen mechanism involving depletion of surface oxygen atoms [31–34], is the only product representing the number of active redox sites.

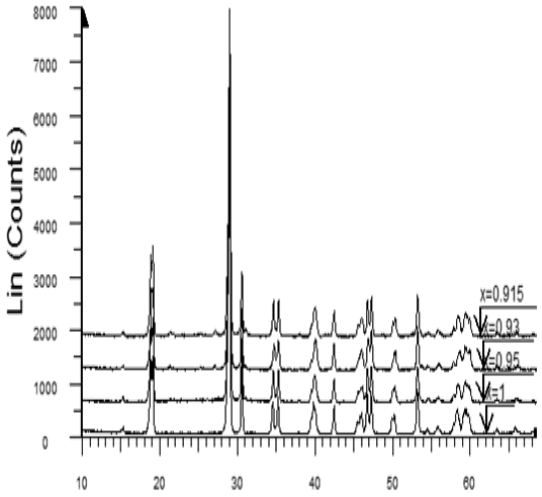

Fig. 3: X-ray diffraction spectra of unsupported $BiP_{1-x}V_xO_4$ catalysts isotype to $BiVO_4$ [21].

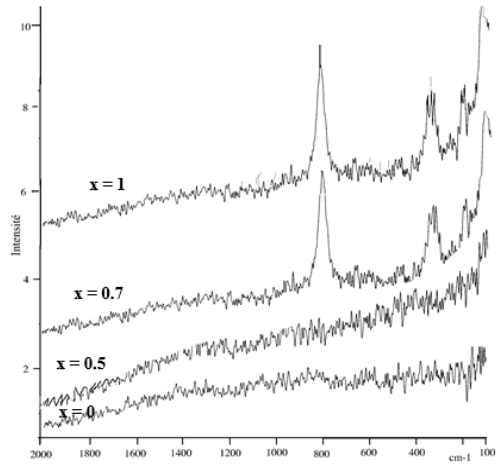

Fig. 4: Raman spectra of $BiP_{1-x}V_xO_4/SiO_2$ catalysts.

As already mentioned above, the $BiPO_4$ catalyst has a very high selectivity for dimethyl ether during the oxidation of methanol, which is attributed to the presence of strong acidic bronsted sites. The absence of the formation of this product in the case of the $BiPO_4$ catalyst supported on silica results from the disappearance of the acidity of the catalyst during the impregnation on silica. It should also be mentioned that a decrease in the strength of the basic sites in the species present and an increase in the redox sites are related to the increase in the vanadium content. Thus, a maximum of redox sites was obtained in the species with x =1, whose $BiVO_4$ phases are dispersed.

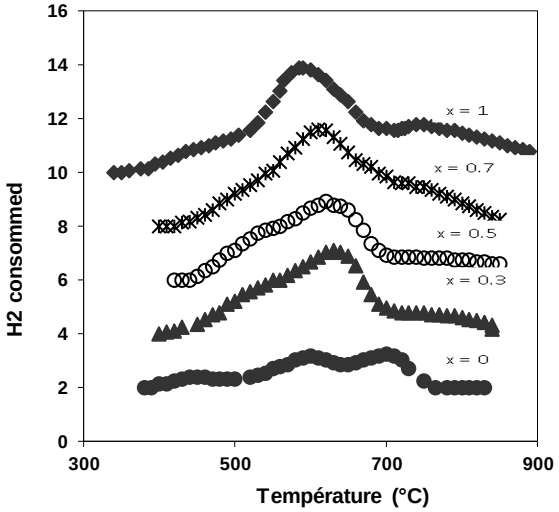

Fig. 5: TPR Profiles of Silica supported $BiP_{1-x}V_xO_4$ Catalysts.

On the other hand, these redox sites decreased with the formation of V_2O_5 for x = 0.3 and x = 0.5.

On the other hand, the most accurate characterization will be obtained for catalysts with only one type of active sites; the spreading effect due to the different types of sites could completely mask the variations in catalytic behavior. The possible transformation of the catalyst surface by the reaction and the need for a small number of different types of active sites are the main limitations of using methanol as a catalytic surface probe. In all other cases, this indirect surface characterization provides relevant information about the behavior of the catalyst surface, allowing an effective comparison of a series of supported and unsupported catalysts. Catalyst surface characterization is complementary to other usual characterization techniques (Raman spectroscopy, X-ray diffraction) and seems to be able to provide the dynamics of the catalyst surface [20].

Catalytic activity

The catalytic results of $BiP_{1-x}V_xO_4/SiO_2$ catalysts in the oxidative dehydrogenation of propane are shown in Table III. The main products were propylene, acrolein, ethylene and CO_2. Increasing the vanadium content leads to an increase in the selectivity of propylene and acrolein (Fig. 6). $BiP_{0.5}V_{0.5}O_4/SiO_2$ samples show better catalytic performance in terms of propylene and acrolein productivity with low activity, one could think of the presence of largeV_2O_5 crystallites, confirmed by XRD. For x ≥ 075, the acrolein selectivity decreases in favor of propylene explained by the presence of $BiVO_4$ species

Table II: Methanol oxidation on $BiP_{1-x}V_xO_4/SiO_2$ series
Reactions conditions: T = 250°C, $CH_3OH/O_2/He$ = 7.1/15.5/77.4 (mol%).

x	Aire spécifique (m^2/g)	S_{DME} (%)	S_F (%)	S_{FM} (%)	S_M (%)	S_{CO2} (%)	Activité globale (mmol/h/g)	(mmol/h/m^2)
Silica	320	0.1	20	24	0.2	55	-	-
0	291.6	2.4	8.8	20.6	4.1	64.1	1.8	0.006
0.1	274	1.6	30.9	34.1	1.6	31.9	3.7	0.0135
0.3	261.6	2.1	40.9	32.4	2.3	22.3	4.6	0.0175
0.5	259	2.2	45.9	33	3.9	15	4.4	0.017
0.7	253	2.9	55.3	24.7	4.1	13	3.3	0.013
0.9	253	3.3	52.5	26.4	3.4	14.4	3.7	0.015
1	254	1	80.1	12	3.2	3.7	6.8	0.027

DME: dimethyle ether, F: formaldehyde, FM: mehylformate, M: methylal.

confirmed by X-ray. The global catalytic activity passes through a maximum at x = 0.9. Moreover, pure $BiPO_4/SiO_2$ shows a very low activity compared to the samples containing vanadium, thus confirming that the catalytic activity of the catalysts is related to the presence of vanadium species. On the other hand, the $BiP_{1-x}V_xO_4/SiO_2$ catalysts with x > 0 convert propane into propylene and acrolein. The preponderance of these products depends on the structure of the species dispersed on the silica and the nature of the active sites [35]. It has been proposed in similar work that isolated tetrahedral vanadium species exhibit greater selectivity for propene than octahedral vanadium species (isolated or associated) [36–40]. This may explain why the catalysts with x=0.3 and x = 0.5, which possess V_2O_5 species show higher selectivity for lower propene than the catalysts with x > 0.7 which possess mainly $BiVO_4$ (tetrahedral VO_4) species. The molecular structures of surface vanadium species on metal oxide supports have been reported in the literature [41–44]. In addition to the catalyst structure, the oxygen bond strength in the surface VO_x species is a primary parameter that governs the activities and selectivities of silica-supported vanadium catalysts. In extensive structural studies [45,46] of supported vanadium oxide catalysts, three types of network oxygen bonds have been identified (Fig. 1): (a) V=O terminal bonds, (b) V-O-V bridging bonds, and (c) V-O-V bridging bonds. Each type of oxygen in the network has different properties.

The studies aimed to determine which type of lattice oxygen binding is responsible for the oxidation activity, which occurs in various catalytic oxidation reactions [47]. It was determined that the V-O-support bond oxygen, rather than the V=O or V-O-V terminal bonds, is the one involved in this catalytic oxidation. This indicates the existence of a weaker interaction between $BiP_{1-x}V_xO_4$ ($x \leq 0.3$) and SiO_2 compared to that between $BiP_{1-x}V_xO_4$ and SiO_2 ($x \geq 0.5$). The increase in activity and selectivity found for the $x \geq 0.5$ catalysts is probably due to the creation of new active sites on the supported $BiP_{1-x}V_xO_4/SiO_2$ layer. These arguments allow us to deduce that the SiO_2 surface carries two types of active sites, namely, (reduced sites and Omega sites (stretched siloxane bridges) which are effective in activating O_2 and propane molecules respectively. $BiPO_4$, V_2O_5 and $BiVO_4$ species present on the silica surface (results X-rays) can all partially mask the active sites on the precipitated SiO_2 surface, with the difference that V_2O_5 and $BiVO_4$ generate its own reduced active sites capable of activating oxygen in the gas phase. On the contrary, we observe that a particular interaction pathway between $BiPO_4$ and SiO_2 has been explained by an encapsulation of $BiPO_4$ in SiO_2 that causes the hydrothermal structural changes of SiO_2 and the formation of hardly reducible species [48]. This statement could explain the inability of silica-supported $BiPO_4$ to promote the formation and stabilization of its own reduced sites. The opposite effect exerted by $BiPO_4$ on the reactivity of bare SiO_2 and in particular in the oxygen activation process has already been correlated with the density of reduced sites determined RTP-H_2. Finally, it is concluded that the activity observed with bare SiO_2 is due to some specific surface sites possessing donor properties to activate molecular oxygen. These sites are negatively influenced by the presence of $BiPO_4$, probably due to physical masking of the sites, but for V_2O_5 and $BiVO_4$ species dispersed on the silica surface for $x \geq 0.5$ catalysts, an appreciable increase in activity and selectivity is made

Table III: Product distribution in ODH of propane over $BiP_{1-x}V_xO_4/SiO_2$ catalysts. T = 480°C, C3H8/O2/He = 10/10/80 (mol%).

x	Conv (%)	$S_{propène}$ (%)	$S_{acrolèine}$ (%)	S_{CO2} (%)	$S_{ethylène}$ (%)	Activité globale (mmol/h/g)	(mmol/h/m2)
0	3	10	13	61	14	0.26	0.0009
0.1	7	16	19	54	11	0.67	0.0024
0.3	9	18	21	53	10	0.89	0.0034
0.5	6	28	31	28	14	0.61	0.0023
0.7	11	23	24	44	12	1.17	0.0046
0.9	16	29	22	38	12	1.66	0.0066
1	16	34	19	37	10	1.57	0.0062

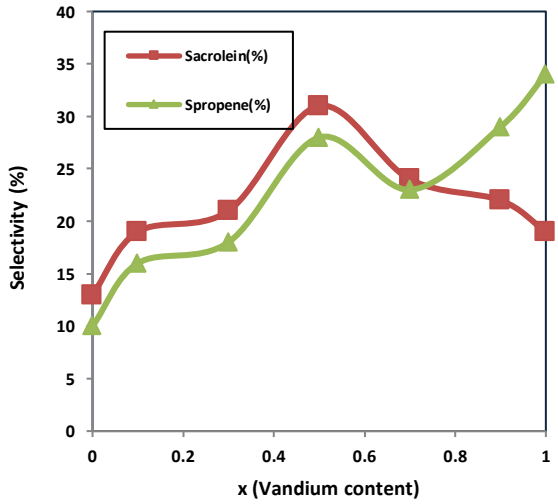

Fig. 6: Evolution of the Selectivity to propylene and acrolein with different vanadium Contents in the propane oxidation.

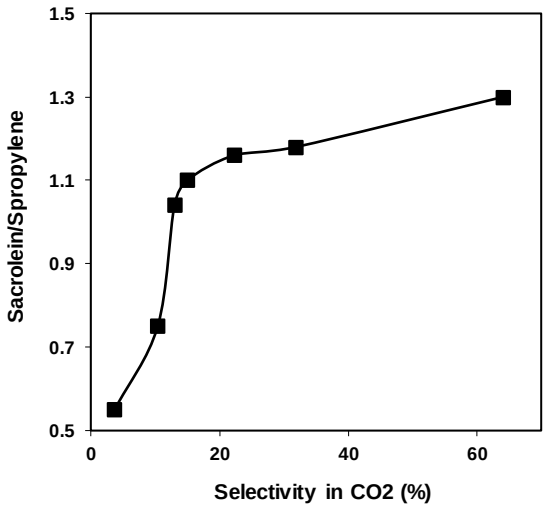

Fig. 7: Correlation between the ratio(S_{C3H4O}/S_{C3H6}) and the CO_2.

possible by the introduction of additional specific reducible sites. A thorough understanding of the precise nature of the sites awaits the results of further surface characterization studies.

According to previously reported data on vanadium catalysts, a correlation between active site reducibility and catalytic activity for oxidation reactions is generally observed [42,48]. In our case, the TPR results indicate that the reducibility of vanadium species increases in the trend or the amount of vanadium increases in the catalysts. However, although the catalytic activity per gram of catalyst shows a similar trend as above, the catalytic activity increases when x (amount of vanadium) increases. This could indicate that a parallelism between catalytic activity and reducibility is observed.

Thus, during the oxidation of propane over $BiP_{1-x}V_xO_4$ / SiO_2 catalysts, acrolein is the main product for highly basic catalysts. While for less basic (redox) catalysts, the selectivity to propylene is higher. Fig. 7 shows the correlation between basicity and acrolein formation, respectively, for $BiP_{1-x}V_xO_4/SiO_2$ catalysts (with basicity estimated by carbon dioxide selectivity in methanol oxidation). An increase in the Sacrolein / Spropylene ratio was observed with increasing basicity.

A correlation could be made with the results obtained by SOKOLOVSKII in the presence of silica solids [49,50]. Indeed, this actor showed that a modification of the silica with an acid leads mainly to the formation of propylene, while with a base, acrolein is obtained (Fig. 8).

This observation regarding the relationship between acrolein production and the basicity of the present catalyst is not supported by several studies [49,50], which found

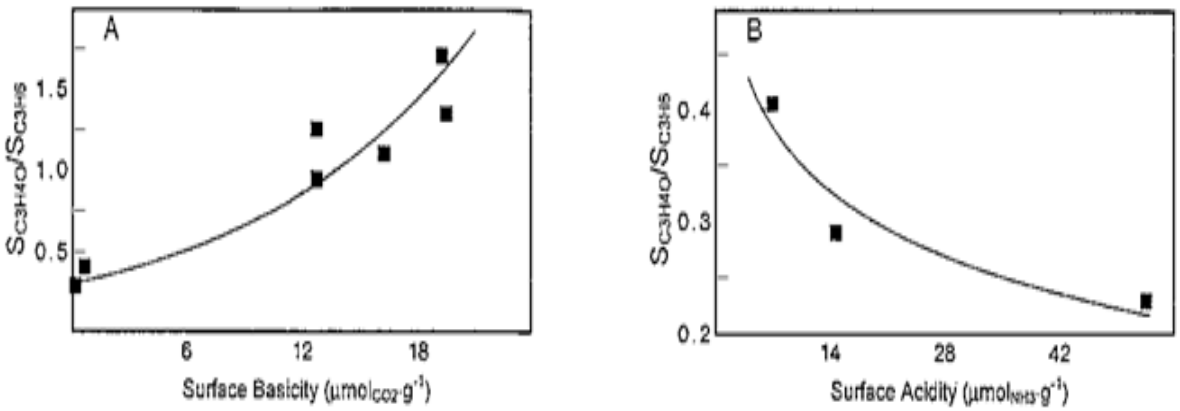

Fig. 8: Correlation between the ratio (S_{C3H4O}/S_{C3H6}) and the surface of SiO_2 modified by an acid and a base [49,50].

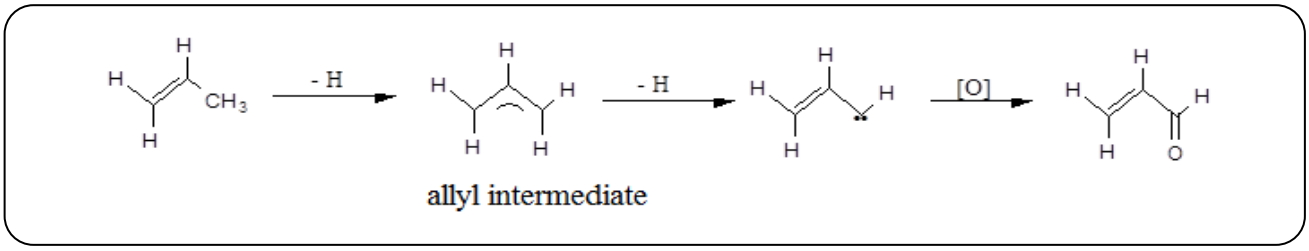

Fig. 9: Reaction mechanism of acrolein formation.

that a basic surface facilitates propylene desorption and increases selectivity. However, it is likely that activation of a propylene occurs at the basic sites of the catalyst, giving an allyl species. On the other hand, silica can create an active oxygen with electrophilic character that can easily interact with the electron-rich allyl species leading to the formation of oxygenated products. Allyl oxidation generally occurs at a site with a center and labile oxygens in an acidic environment: the acid stabilizes the propylene by interaction between the electrons of the double bond and a metal cation (Lewis acid site), which induces eventual abstraction of H from the -CH_3 moiety and, thus, leads to the formation of allyl intermediate. The removal of a second H, and the incorporation of oxygen leads to acrolein (Fig. 9).

According to Grasselli [51,52], the initial removal of a hydrogen on the simple binary system of the Bi-P-V-O oxide involves an oxygen associated with bismuth and leads to an allyl intermediate, which is probably a free radical in nature. Grasselli then suggests that this intermediate is then rapidly trapped by complexing with the V^{5+} centers to give an allyl species. This species is symmetric in the sense that the carbon atoms at position 1 and 3 have the same probability of carrying the aldehyde function. The next step is the formation of a bond between the terminal allyl carbon and the oxygen of a nucleophilic center (allyl oxo bonded complex). Removal of the second hydrogen involves a nucleophilic center, resulting in the reduction of vanadium and desorption of acrolein. The catalyst is then regenerated by molecular oxygen as a result of dissociative adsorption onto centers different from the previous ones and subsequent migration to the olefin oxidation sites.

However, it is necessary to emphasize that the rate of a reaction and the distribution of products of an alkane oxidation depend on the acid-base properties of a catalyst [53,54]. In our case, it is clear that the strong base region is attributed to a fast reaction. Therefore, it can be concluded that the acid-base character of a catalyst controls the rate of a specific reaction and the distribution of the products of the ODH reaction of propane. Basicity increases the rate of the reaction, so that acrolein is formed. On the other hand, the acidity of the catalyst decreases the rate of reaction, resulting in the formation of the main product of the ODH reaction, which is propylene.

CONCLUSIONS

The activities and selectivity's of the propane ODH reaction depend significantly on the structures of the V_2O_5, $BiPO_4$ and $BiVO_4$ species present on the silica support. With increasing V contents, the structures present on the support evolve from $BiPO_4$ to isolated $BiVO_4$ through V_2O_5 crystallites. Isolated $BiVO_4$ and V_2O_5 are more active due to their higher reducibility, whereas $BiPO_4$ crystallites are significantly less selective for propylene and acrolein in propane ODH. This superiority of $BiVO_4$ crystallites in propylene and acrolein formation is consistent with their reducible properties, and the presence of redox sites confirmed by methanol oxidation. This reaction is a very sensitive method for detecting very small changes in the nature of the catalytically active phase of $BiP_{1-x}V_xO_4$ /SiO_2 catalysts. Any structural modification of the catalytic site generally leads to an observable evolution of the selectivity. This study provides fundamental information useful for the design and construction of supported $BiP_{1-x}V_xO_4$ catalysts with desirable crystal structures for efficient production of propylene and acrolein from propane ODH. These new results provide fundamental information on the molecular structure-redox site-reactivity/selectivity relationships of molecularly dispersed SiO_2 supported oxides.

Received : Oct. 29, 2021 ; Accepted : Jan. 31, 2022

REFERENCES

[1] Kaddouri A., Mazzocchia C., Tempesti E., The Synthesis of Acrolein and Acrylic Acid by Direct Propane Oxidation with Ni-Mo-Te-P-O Catalysts, *Appl. Catal. A Gen.*, **180**:271–275 (1999).

[2] Chen L., Liang J., Lin H., Weng W., Wan H., Védrine J.C., MCM41 and Silica Supported Movte Mixed Oxide Catalysts for Direct Oxidation of Propane to Acrolein, *Appl. Catal. A Gen.*, **293**:49–55 (2005).

[3] Yahya G., Sagir A., Abdulrahman A. R.L., Catalyst Design and Tuning for Oxidative dehydrogenation of Propane - A review, *Appl. Catal. A, Gen.*, **20**:1–100 (2020).

[4] Zhang X., Wan H., Weng W., Reaction pathways for Selective Oxidation of Propane To Acrolein over Ce-Ag-Mo-P-O Catalysts, *Appl. Catal. A Gen.*, **353**: 24–31 (2009).

[5] Andrushkevich T. V., Popova G.Y., Chesalov Y.A., Ischenko E.V., Khramov M.I., Kaichev V. V., Propane Ammoxidation on Bi Promoted MoVTeNbOx Oxide Catalysts: Effect of Reaction Mixture Composition, *Appl. Catal. A Gen.*, **506**: 109–17 (2015).

[6] Fan X., Zhang H., Li J., Zhao Z., Xu C., Liu J., Duan A., Jiang G., Wei Y., Ni-Mo Nitride Catalysts: Synthesis and Application in the Ammoxidation of Propane, *Chinese J. Catal.*, **35**: 286–93 (2014).

[7] Wang Y., Ma F., Chen S., Chen F., Lu W.M., Performance of Mo-V-Te-P Catalysts Supported on the SiC for Propane Selective Oxidation to Acrolein, *Chinese Chem. Lett.*, **22**: 1321–1325 (2011).

[8] Ouchabi M., Agunaou M. M.B., Oxydeshydrogenation du Propane Sur Des Catalyseurs $BiP_{1-x}V_xO_4$, *Ann. Chim. Sci. des Mater.*, **26**:497–503 (2001).

[9] Liu G., Zhao Z.J., Wu T., Zeng L., Gong J., On the Nature of Active Sites of VO_x/Al_2O_3 Catalysts for Propane Dehydrogenation, *ACS Catal.*, **6**: 5207–5214 (2016).

[10] Miranda G.P., Ferreira Neto V.J.M., Young A.F., Silveira E.B., Pries de Oliveira P.G., Mendes F.M.T., Oxidative dehydrogenation of Propane: Developing Catalysts Containing VO_X, V-P-O and V-Mg-O Species Supported on MCM-41 and Activated Carbon, *Catal. Today*, **348**:148–56 (2020).

[11] Hu J., Lu Z., Yin H., Xue W., Wang A., Shen L., Liu S., Aldol Condensation of Acetic Acid with Formaldehyde to Acrylic Acid over SiO_2-, SBA-15-, and HZSM-5-Supported V-P-O Catalysts, *J. Ind. Eng. Chem.*, **40**: 145–151 (2016).

[12] Solyntjes S., Neumann B., Stammler H.G., Ignat'ev N., Hoge B., Bismuth Perfluoroalkylphosphinates: New Catalysts for Application in Organic Syntheses, *Chem. - A Eur. J.*, **23**:1568–75 (2017).

[13] Zazhigalov V.A., Bogutskaya L.V, Bacherikova I.V., Kharlamov A.I., Stoch J., Mechanochemical Modification of V-P-Bi-O Catalysts, *Theor. Exp. Chem.*, **31**: 258–260 (1995).

[14] Xie Y., Luo R., Sun G., Chen S., Zhao Z.J., Mu R., Gong J., Facilitating the Reduction of V-O Bonds on VOx/ZrO_2 Catalysts for Non-Oxidative Propane Dehydrogenation, *Chem. Sci.*, **11**: 3845–51 (2020).

[15] Einaga H., Maeda N., Yamamoto S., Teraoka Y., Catalytic Properties of Copper-Manganese Mixed Oxides Supported on SiO_2 for Benzene Oxidation with Ozone, *Catal. Today*, **245**: 22–7 (2015).

[16] Yang K., Zhang Y., Li Y., Huang P., Chen X., Dai W., Fu X., Insight Into the Function of Alkaline Earth Metal Oxides as Electron Promoters for Au/TiO_2 Catalysts Used in CO Oxidation, *Appl. Catal. B Environ.*, **183**:206–15 (2015).

[17] Damma D., Boningari T., Ettireddy P.R., Reddy B.M., Smirniotis P.G., Direct Decomposition of NO_x over TiO_2 Supported Transition Metal Oxides at Low Temperatures, *Ind. Eng. Chem. Res.*, **57**:615–44 (2018).

[18] Wang L., Wan H., Jin S., Chen X., Li C., Liang C., Hydrodeoxygenation of Dibenzofuran over SiO_2, Al_2O_3/SiO_2 and ZrO_2/SiO_2 Supported Pt Catalysts, *Catal. Sci. Technol.*, **5**:465–74 (2014).

[19] Vessally E., Farajzadeh P., Najafi E., Possible Sensing Ability of Boron Nitride Nanosheet and its Al– and Si–Doped Derivatives for Methimazole Drug by Computational Study, *Iran. J. Chem. Chem. Eng. (IJCCE)*, **40(4)** :1001–11 (2021).

[20] Tatibouet J.M., Methanol Oxidation as a Catalytic Surface Probe, *Appl. Catal. A Gen.*, **148**:213–52 (1997).

[21] AGUNAOU M., OUCHABI M., Synthesis and Characterization of Nano-Structured Mixed Oxides, *Ann. Chim. Sci. des Matériaux*, **25**:17–20 (2000).

[22] Ding C., Han A., Ye M., Zhang Y., Yao L., Yang J., Hydrothermal Synthesis and Characterization of Novel Yellow Pigments Based on V^{5+} Doped $BiPO_4$ with High Near-Infrared Reflectance, *RSC Adv.*, **8**:19690–700 (2018).

[23] Li X., Li F., Lu X., Zuo S., Li Z., Yao C., Ni C., Microwave Hydrothermal Synthesis of $BiP_{1-x}V_xO_4$/Attapulgite Nanocomposite with Efficient Photocatalytic Performance for Deep Desulfurization, *Powder Technol.*, **327**:467–75 (2018).

[24] Van Lingen J.N.J., Gijzeman O.L.J., Weckhuysen B.M., Van Lenthe J.H., On the Umbrella Model for Supported Vanadium Oxide Catalysts, *J. Catal.*, **239**:34–41 (2006).

[25] Pak C., Bell A.T., Tilley T.D., Oxidative dehydrogenation of Propane over Vanadia-Magnesia Catalysts Prepared by Thermolysis of $OV(OtBu)_3$ in the Presence of Nanocrystalline MgO, *J. Catal.*, **206**:49–59 (2002).

[26] Au C.T., Zhang W.D., Wan H.L., Preparation and Characterization of Rare Earth Orthovanadates for Propane Oxidative dehydrogenation, *Catal. Letters*, **37**:241–6 (1996).

[27] Deo G., Hardcastle F.D., Richards M., Hirt A.M., Wachs I.E., Raman Spectroscopy of Vanadium Oxide Supported on Alumina, *Novel Materials in Heterogeneous Catalysis*, pp.317–28 (1990).

[28] Bosch H., Kip B.J., Van Ommen J.G., Gellings P.J., Factors Influencing the Temperature-Programmed Reduction Profiles of Vanadium Pentoxide, *J. Chem. Soc. Faraday Trans. 1 Phys. Chem. Condens. Phases*, **80**:2479–88 (1984).

[29] Klisińska A., Samson K., Gressel I., Grzybowska B., Effect of Additives on Properties of V_2O_5/SiO_2 and V_2O_5/MgO Catalysts. I. Oxidative dehydrogenation of Propane and Ethane, *Appl. Catal. A Gen.*, **309**: 10–6 (2006).

[30] Yavari Z., Noroozifar M., Mirghoreishi Roodbaneh M., Ajorlou B., $SrFeO_{3-\delta}$ Assisting with Pd Nanoparticles on the Performance of Alcohols Catalytic Oxidation, *Iran. J. Chem. Chem. Eng. (IJCCE)*, **36(6)**: 21–37 (2017).

[31] Yun D., Wang Y., Herrera J.E., Ethanol Partial Oxidation over VO_x/TiO_2 Catalysts: The Role of Titania Surface Oxygen on Vanadia Reoxidation in the Mars-van Krevelen Mechanism, *ACS Catal.*, **8**:4681–93 (2018).

[32] Nair H., Baertsch C.D., Method for Quantifying Redox Site Densities in Metal Oxide Catalysts: Application to the Comparison of Turnover Frequencies for Ethanol Oxidative dehydrogenation over Alumina-Supported VO_x, MoO_x, and WO_x Catalysts, *J. Catal.*, **258**:1–4 (2008).

[33] Nair H., Gatt J.E., Miller J.T., Baertsch C.D., Mechanistic Insights into the Formation of Acetaldehyde And Diethyl Ether From Ethanol over supported VO_x, MoO_x, and WO_x catalysts, *J. Catal.*, **279**:144–54 (2011).

[34] Wachs I.E., Routray K., "Catalysis Science of Bulk Mixed Oxides", American Chemical Society, (2012).

[35] Zhang S., Liu H., Oxidative dehydrogenation of Propane over Mg-V-O Oxides Supported on MgO-Coated Silica: Structural Evolution and Catalytic Consequence, *Appl. Catal. A Gen.*, **573**:41–8 (2019).

[36] Lindblad T., Rebenstorf B., Yan Z.G., Andersson S.L.T., Characterization of Vanadia Supported on Amorphous $AlPO_4$ and its Properties for Oxidative Dehydrogenation of Propane, *Appl. Catal. A, Gen.*, **112**:187–208 (1994).

[37] Parmaliana A., Arena F., Sokolovskii V., Frusteri F., Giordano N., A Comparative Study of the Partial Oxidation of Methane to Formaldehyde on Bulk and Silica Supported MoO_3 and V_2O_5 Catalysts, *Catal. Today*, **28**:363–71 (1996).

[38] Grabowski R., Kinetics of Oxidative dehydrogenation of C2 -C3 Alkanes on Oxide Catalysts, *Catal. Rev. Sci. Eng.*, **48**:199–268 (2007).

[39] Chen K., Khodakov A., Yang J., Bell A.T., Iglesia E., Isotopic Tracer and Kinetic Studies of Oxidative dehydrogenation Pathways on Vanadium Oxide Catalysts, *J. Catal.*, **186**:325–33 (1999).

[40] Chen K., Xie S., Bell A.T., Iglesia E., Structure and Properties of Oxidative dehydrogenation Catalysts Based on MoO_3/Al_2O_3, *J. Catal.*, **198**:232–42 (2001).

[41] Wu Z., Kim H.S., Stair P.C., Rugmini S., Jackson S.D., On the Structure of Vanadium Oxide Supported on Aluminas: UV and Visible Raman Spectroscopy, UV-Visible Diffuse Reflectance Spectroscopy, and Temperature-Programmed Reduction Studies, *J. Phys. Chem. B*, **109**:2793–800 (2005).

[42] Argyle M.D., Chen K., Bell A.T., Iglesia E., Effect of Catalyst Structure on Oxidative Dehydrogenation of Ethane and Propane on Alumina-Supported Vanadia, *J. Catal.*, **208**:139–49 (2002).

[43] Klose F., Wolff T., Lorenz H., Seidel-Morgenstern A., Suchorski Y., Piórkowska M., Weiss H., Active Species on γ-Alumina-Supported Vanadia Catalysts: Nature and Reducibility, *J. Catal.*, **247**:176–93 (2007).

[44] Murgia V., Sham E., Gottifredi J.C., Torres E.M.F., Oxidative dehydrogenation of Propane and N-Butane over Alumina Supported Vanadium Catalysts, *Lat. Am. Appl. Res.*, **34**:75–82 (2004).

[45] Wachs I.E., Jehng J.M., Deo G., Weckhuysen B.M., Guliants V.V., Benziger J.B., In Situ Raman Spectroscopy Studies of Bulk and Surface Metal Oxide Phases During Oxidation Reactions, *Catal. Today*, **32**:47–55 (1996).

[46] Wachs I.E., Weckhuysen B.M., Structure and Reactivity of Surface Vanadium Oxide Species on Oxide Supports, *Appl. Catal. A Gen.*, **157**:67–90 (1997).

[47] Goutam Deo I.E.W., Reactivity of Supported Vanadium Oxide Catalysts: The Partial Oxidation of Methanol, *J. Catal.*, **146**:323–34 (1994).

[48] Dai H., Bell A.T., Iglesia E., Effects of Molybdena on the Catalytic Properties of Vanadia Domains Supported on Alumina for Oxidative dehydrogenation of Propane, *J. Catal.*, **221**:491–9 (2004).

[49] Parmaliana A., Arena F., Frusteri F., Giordano N., Scurrell M.S., Sokolovskii V., Partial oxidation of Methane to Formaldehyde on Bulk and Silica Supported MoO3 and V_2O_5 Catalysts: Surface Features and Reaction Mechanism, *Stud. Surf. Sci. Catal.*, **107**: 23–28 (1997).

[50] Miceli D., Arena F., Parmaliana A., Scurrell M.S., Sokolovskii V., Effect of the Metal Oxide Loading on the Activity of Silica Supported MoO_3 and V_2O_5 Catalysts in the Selective Partial Oxidation of Methane, *Catal. Letters*, **18**:283–8 (1993).

[51] Stern D.L., Grasselli R.K., Reaction Network and Kinetics of Propane Oxydehydrogenation over Nickel Cobalt Molybdate, *J. Catal.*, **167**:560–9 (1997).

[52] Grasselli R.K., Burrington J.D., Brazdil J.F., Mechanistic Features of Selective Oxidation and Ammoxidation Catalysis, *Faraday Discuss. Chem. Soc.*, **72**:203–23 (1981).

[53] Burch R., Hayes M.J., C-H Bond Activation in Hydrocarbon Oxidation on Solid Catalysts, *J. Mol. Catal., A. Chem.*, **100**:13–33 (1995).

[54] Sokolovskii V., Arena F., Giordano N., Parmaliana A., Role of Acid-Base Properties of SiO_2-Based Catalysts in the Selective Oxidation of Propane, *J. Catal.*, **167**:296–9 (1997).